Gallium-Labeled Deferoxamine-Galactosyl-Neoglycoalbumin: A Radiopharmaceutical for Regional Measurement of Hepatic Receptor Biochemistry

David R. Vera

Division of Nuclear Medicine, Department of Radiology, University of California, Davis, Medical Center, Sacramento, California

Galactosyl-neoglycoalbumin (NGA) is a synthetic ligand to the hepatocyte-specific receptor, hepatic binding protein. In-vitro and in-vivo characterization of a chelation-based derivative of NGA, deferoxamine-galactosyl-neoglycoalbumin (DF-NGA), is described. A two-step glutaraldehyde method was used to covalently couple deferoxamine (DF) to NGA. Products with an average DF-to-NGA ratio of less than 2 contained less than 3% polymeric DF-NGA. All products retained the chelator after 12 mo of storage at 4°C. Gallium labeling of DF-NGA-41 (41 galactose units per HSA) with an average of 1.1 DF per NGA was quantitative within 15 min after the addition of ^{67}Ga-citrate. The labeled product was stable for at least 24 hr. Scatchard and reverse-binding assays of ^{67}Ga-DF-NGA-41 revealed a forward binding rate constant k_b similar to that of ^{125}I-NGA-44. The %ID of ^{67}Ga-DF-NGA-41 in rabbit liver was approximately 90% at 10 min after injection of 1.2×10^{-9} mole DF-NGA per kilogram of body weight. This value decreased to 40% at a scaled molar dose of 1.2×10^{-7} mol/kg. Biodistribution data of ^{67}Ga-DF-NGA in rabbits was similar to ^{99m}Tc-NGA. High tissue specificity and facile labeling will make ^{68}Ga-labeled neoglycoalbumin an ideal agent for regional measurements of receptor biochemistry in the investigational and clinical setting.

J Nucl Med 1992; 33:1160–1166

Technetium-99m-galactosyl-neoglycoalbumin (NGA) (*1*) is a receptor-binding radiopharmaceutical designed for quantitative assessment of hepatic function (*2,3*). Kinetic analysis (*4*) of liver and heart time-activity data following a 30-min dynamic imaging study, provides simultaneous estimates of receptor concentration and affinity that correlate with independent measurements via in vitro radioassay (*5*). This procedure, which employs planar imaging, produces parameters that represent the average receptor concentration within the entire liver, and similarly, the average receptor affinity. Use of NGA as a quantitative tool for in vivo studies of hepatic physiology will require regional measurement of receptor concentration and affinity. For this purpose, we have developed a NGA-derivative suitable for PET.

Preliminary work (*6*) was conducted to test the feasibility of a ^{68}Ga-labeled NGA and kinetic modeling of ^{68}Ga-NGA PET observations. We reported high labeling yields and proposed a regional kinetic model using PET observations. This current report describes the synthesis, labeling, and biodistribution of deferoxamine-conjugated NGA. Coupling was accomplished by a two-step glutaraldehyde method introduced by Yokoyama et al. (*7*). This method provided a NGA conjugate which was stable during long-term storage. Our previous report utilized a carbodiimide-mediated coupling reaction, which did not provide a stable conjugate and consequently poor labeling yields after storage.

MATERIALS AND METHODS

Deferoxamine Conjugation

Human serum albumin (HSA) (Travenol Laboratories; Glendale, CA) was separated from stabilizers and preservatives by diafiltration with 10 exchange volumes of 0.9% saline in an ultrafiltration cell (YM30 membrane, Amicon Corp.; Danvers, MA). Protein concentration was determined by ultraviolet absorbance (280 nm) with HSA as the standard. NGA was prepared by covalently coupling 2-imino-2-methoxyethyl-1-thio-β-D-galactopyranoside as previously described (*1*). Monomeric HSA and NGA were isolated by gel chromatography (Sephadex G-200, Pharmacia Fine Chemicals, Piscataway, NJ) using 0.9% saline as the mobile phase. Measurement of the NGA carbohydrate density (*1*) had a relative error of 8%.

Conjugation of deferoxamine (DF) to NGA or HSA was achieved by the two-step method described by Yokoyama et al. (*7*). The reaction product was filtered (0.2 μm) into an ultrafiltration cell (YM30 membrane) and diafiltered with ten exchange volumes of 0.9% saline at 4°C to remove any unconjugated DF. The DF-NGA was then concentrated to 10 mg/ml and stored at

Received Apr. 17, 1991; revision accepted Jan. 31, 1992.

For reprints contact: David R. Vera, PhD, Division of Nuclear Medicine, Dept. of Radiology, University of California, Davis, Medical Center, 2315 Stockton Blvd., Sacramento, CA 95817.

4°C. Size exclusion chromatography (TSK-3000SW, 1 ml/min 0.9% saline, Beckman Instruments, Palo Alto, CA) was performed immediately after purification and after various lengths of storage. Elution volumes were: polymeric DF-NGA, 6.0 ml; dimeric DF-NGA, 8.2 ml; monomeric DF-NGA-41, 9.6 ml; DF-HSA, 9.9 ml.

The average number of deferoxamine units per protein molecule was determined by the measurement of protein and DF concentration. The deferoxamine was assayed by the method of Emery and Hoffer (*8*) as modified by Yokoyama et al. (*7*). The relative error of the assay was 2%. The average number of DF molecules per protein molecule was then calculated as the ratio of DF and protein concentrations.

Gallium-67 Labeling

The labeling of DF-NGA with ^{67}Ga required the simple addition of ^{67}Ga-citrate to DF-NGA in 0.9% saline. A standard protocol was used to label DF-NGA at the same product concentration (5 mg/ml) as ^{99m}Tc-NGA (*1*). Up to 0.5 ml (~1 mCi) of ^{67}Ga-citrate (DuPont, N. Billerica, MA) was added to 5 mg of DF-NGA (0.5 ml). After addition of 100 μl 0.25 *M* sodium bicarbonate and 0.9% saline to supplement the reaction volume to 1 ml, the product was allowed to stand for at least 15 min. Size-exclusion chromatography (Sephadex G-25, Superfine, 10 × 100 mm, HR 10/10, Pharmacia-LKB, Piscataway, NJ; 1 ml/min 0.9% saline, 50 μl sample) with radioactivity (100–1000 keV) detection, was used to assay labeling yield and stability. Analysis of chromatographic data was performed by standard software (System Gold, Beckman Instruments, Palo Alto, CA). Elution volumes were: ^{67}Ga-DF-NGA, 2.5 ml; ^{67}Ga-DF, 5.4 ml; and ^{67}Ga-citrate, 9.8 ml. Typical recoveries within three times the column's bed volume were in excess of 98% for individual applications of ^{67}Ga-DF-NGA (column-purified), ^{67}Ga-DF, ^{67}Ga-citrate and the ^{67}Ga-DF-NGA reaction product. Labeling yield was defined as the integral of the ^{67}Ga-DF-NGA activity peak divided by the integral of the ^{67}Ga-DF-NGA, ^{67}Ga-DF and ^{67}Ga-citrate peaks.

Binding and Biodistribution Assays

Scatchard and reverse binding assays were performed as previously described (*9*) using ^{67}Ga-DF-NGA-41 (0.70 DF/HSA). Separation of membrane-bound from free ^{67}Ga-DF-NGA was achieved by the application of the entire assay volume (500 μl) to a 0.45-μm filter (HVLP 013, Millipore Corp., Bedford, MA) (previously soaked in assay buffer containing 0.1% DF-HSA), assembly (MPS 1, Amicon, Danvers, MA) and centrifuged (High-Speed Centrifuge with Model HSR-16 rotor, Savant Instruments, Farmingdale, NY) at 3600 g for 3 min. The filters were then rinsed and centrifuged three times each with 200 μl of assay buffer.

Biodistribution of ^{67}Ga-DF-NGA was tested in New Zealand White rabbits (2.2–2.7 kg) in the manner previously described (*1*) for ^{99m}Tc-NGA. Briefly, the anesthetized animals were injected in the marginal ear vein with ^{67}Ga-DF-NGA-41 (1.1 DF/NGA) (7.4×10^{-10} mole/kg) followed immediately by a dose of ^{125}I-HSA (0.2–0.3 μCi). Arterial blood was sampled from the central artery of the ear, and the animals were euthanized at 3 or 60 min postinjection. Two animals, one of each sex, were studied at each time point. The liver was removed, weighed and homogenized after all major vessels were clamped and ligated. The remaining organs listed in Table 1 were removed, weighed and dispensed into 20-ml polyethylene scintillation vials. The contents were removed from the stomach, small intestine and large intestine and counted. Standards and samples (corrected for self-absorption) were assayed (200-480 keV) for ^{67}Ga immediately after the study, and ^{125}I (15–80 keV) 14–21 days later.

Dose-dependency kinetics of ^{67}Ga-DF-NGA-41 (1.1 DF/NGA) were studied in New Zealand White rabbits (2.3–3.4 kg) as previously described (*10*). Three studies were performed using one of three scaled molar doses (1.2×10^{-9}, 1.2×10^{-8}, or 1.2×10^{-7} mole/kg) of ^{67}Ga-DF-NGA-41. The lowest dose used a high-specific activity protocol. To facilitate the exchange of possible contaminants with the trivalent gallium (*11*), 100 μl ascorbic acid (3 m*M*) was added to 1 ml ^{67}Ga-citrate (~4 mCi); 100 μl sodium bicorbonate (2.5 m*M*) and 2.5 mg DF-NGA were then added, and the solution was allowed to stand at room temperature for at least 18 hr. Labeling yields were in excess of 95%. Each animal was anesthetized and positioned under a gamma camera (Pho/Gamma IV, Searle Radiographics; Chicago, IL) fitted with a medium-energy (250 keV) collimator. Computer acquisition (ADAC Laboratories) (128 × 128 × 8 byte mode, 15-sec frames, 80 frames) was started immediately upon injection of the ^{67}Ga-DF-NGA (0.4–3.0 mCi). Plasma volume was measured with ^{125}I-HSA (~0.3 μCi) using samples at 3, 15 and 30 min postinjection. Time-activity curves were generated from liver and heart ROIs. These curves were then scaled to percent of injected DF-NGA using the plasma volume and fraction of injected DF-NGA in a 100-μl plasma sample withdrawn 3 min after the ^{67}Ga-DF-NGA injection. This calculation was based on the assumption that DF-NGA not in the plasma at 3 min postinjection was residing in the liver.

Dosimetry

The absorbed radiation dose to various tissues resulting from the administration of ^{68}Ga-DF-NGA into human subjects was calculated. Accumulated activities $\tilde{A}_h$ from blood (total body), liver, small intestine and bladder were based on kinetic equations previously derived for technetium-labeled NGA (*1*) with biodistribution parameters obtained from the mean of six baboon studies (*1*). We assumed that excretion of labeled metabolic products was equally distributed between the urinary and GI tracts. Absorbed doses to liver, small intestine, bladder wall, total body, red marrow, ovaries, uterus and testes were calculated using S-factors for ^{68}Ga (*12*).

RESULTS

Deferoxamine Conjugation

When deferoxamine was covalently coupled to HSA, NGA-18 and NGA-41, the ability of the molecule to conjugate with the deferoxamine was inversely proportional to the galactose density (number of galactose units per albumin molecule) of the protein (Fig. 1). When the preconjugation ratio of deferoxamine to HSA was 300:1, the post-conjugation ratio was 8.0 mol/mol, whereas the NGA-18 and NGA-41 post-conjugation ratios were 4.4 and 1.1 mol/mol, respectively.

Size-exclusion chromatography of DF-HSA (0.7 DF per HSA) and DF-NGA-41 (1.1 DF per HSA) immediately after diafiltration revealed less than 2% polymers in either preparation (Fig. 2). Chromatography, after 1 and 12 mo of storage at 4°C, did not detect free deferoxamine or the

TABLE 1
Rabbit Biodistribution of ^{67}Ga-DF-NGA-41 and ^{125}I-HSA

	Time After Injection (min)							
	3				60			
	^{67}Ga		^{125}I		^{67}Ga		^{125}I	
	ID (%)	ID (% g^{-1})	ID (%)	ID (% g^{-1})	ID (%)	ID (% g^{-1})	ID (%)	ID (% g^{-1})
Liver	71.	0.96	18.	0.25	58.	0.75	18.	0.24
	69.	0.72	18.	0.20	42.	0.50	21.	0.23
Plasma	16.	0.15	100.	0.97	1.7	0.011	100.	0.68
	19.	0.14	100.	0.72	3.7	0.026	100.	0.70
Urine	1.6	—	0.030	—	6.0	—	0.22	—
	0.67	—	0.043	—	7.5	—	0.73	—
Kidneys	0.95	0.055	1.8	0.11	0.25	0.017	2.5	0.15
	0.86	0.053	1.4	0.089	0.44	0.024	3.0	0.16
Urinary bladder	0.047	0.013	0.089	0.025	0.010	0.0062	0.041	0.023
	0.023	0.011	0.042	0.021	0.021	0.0052	0.11	0.032
Small intestine	0.56	0.015	1.7	0.044	2.3	0.058	2.0	0.050
	0.50	0.012	1.2	0.030	2.2	0.050	1.9	0.042
Small intestine contents	0.50	—	0.34	—	7.0	—	0.84	—
	0.26	—	0.34	—	6.9	—	0.77	—
Gallbladder*	0.039	0.050	0.042	0.054	0.223	0.44	0.040	0.079
	0.080	0.054	0.074	0.050	0.014	0.0062	0.062	0.036
Bone, femur	4.3	0.017	12.	0.047	1.0	0.0040	18.	0.069
	4.3	0.016	11.	0.040	1.5	0.0052	14.	0.048
Bone, rib	3.5	0.014	14.	0.054	0.53	0.0021	13.	0.050
	2.2	0.0083	11.	0.042	0.29	0.0012	11.	0.036
Muscle	3.6	0.0035	3.4	0.003	1.0	0.0011	6.7	0.0065
	1.4	0.0030	3.5	0.003	1.3	0.0011	8.9	0.0076
Lung	2.6	0.12	8.7	0.40	0.16	0.0077	7.5	0.34
	1.6	0.068	6.0	0.26	0.17	0.015	2.5	0.22
Spleen	0.034	0.028	0.15	0.12	0.016	0.013	0.092	0.072
	0.037	0.032	0.12	0.10	0.011	0.012	0.12	0.13
Heart	0.34	0.035	2.1	0.21	0.053	0.0045	2.3	0.20
	0.60	0.050	2.5	0.21	0.070	0.010	1.0	0.14
Brain	0.011	0.012	0.072	0.0066	0.0022	0.00022	0.096	0.0096
	0.011	0.012	0.074	0.0075	0.0045	0.00045	0.12	0.012
Stomach	0.34	0.012	0.81	0.028	0.49	0.017	0.70	0.024
	0.27	0.0086	0.48	0.015	0.43	0.010	0.75	0.016
Stomach contents	0.033	—	0.035	—	1.6	—	0.22	—
	0.076	—	0.11	—	0.58	—	0.29	—
Large intestine	0.83	0.010	2.2	0.027	0.18	0.0022	2.5	0.037
	0.54	0.0068	1.3	0.016	0.25	0.0036	2.0	0.026
Large intestine contents	0.20	—	0.073	—	0.070	—	0.26	—
	0.082	—	0.12	—	0.079	—	0.85	—
Thyroid	0.020	0.016	0.091	0.071	0.0031	0.0021	0.082	0.057
	0.015	0.011	0.067	0.046	0.011	0.0062	0.20	0.10
Thymus	0.039	0.0085	0.17	0.037	0.014	0.0022	0.36	0.049
	0.040	0.0090	0.15	0.034	0.028	0.0043	0.33	0.052
Eyes	0.010	0.0020	0.013	0.0021	0.0064	0.0011	0.042	0.0085
	0.0068	0.0013	0.031	0.0063	0.0086	0.0011	0.095	0.015
Testes	—	—	—	—	—	—	—	—
	0.045	0.004	0.094	0.010	0.054	0.005	0.49	0.040
Ovaries	0.0080	0.031	0.023	0.097	0.0021	0.0051	0.091	0.21
	—	—	—	—	—	—	—	—
Injection site	0.025	—	0.10	—	0.015	—	0.041	—
	0.014	—	0.062	—	0.011	—	0.13	—
I.V. line	0.66	—	0.080	—	0.24	—	0.08	—
	0.56	—	3.2	—	0.096	—	0.093	—

* Including contents.

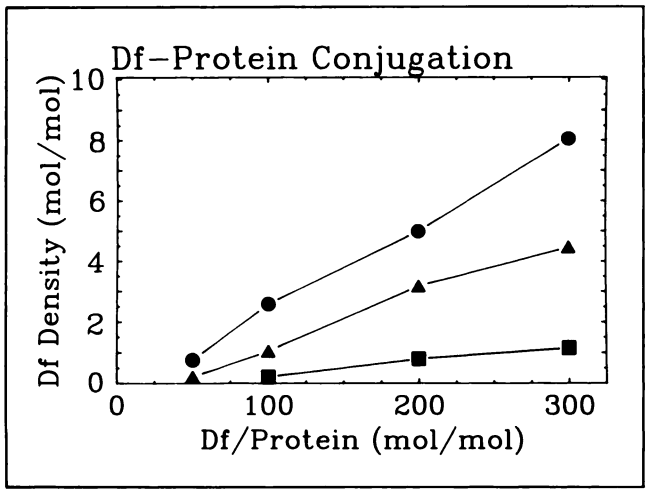

FIGURE 1. Deferoxamine (DF) density, the number of deferoxamine molecules per NGA, was controlled by the molar ratio of the starting reagents (DF and protein) and the carbohydrate density (gal/HSA) of the albumin: albumin without covalently coupled galactose (circles), NGA-18 (18 gal/HSA) (triangles), and NGA-41 (squares).

formation of additional polymer. Products with an average DF-to-NGA ratio of less than 2 contained less than 3% polymeric DF-NGA.

Gallium Labeling

Labeling yields were in excess of 98% as measured by size exclusion chromatography. When repeated 24 hr after labeling, no increase in activity was detected within the citrate or deferoxamine elution volumes.

Scatchard and Reverse Binding

The Scatchard assay of DF-NGA-41 (1.1 DF/NGA) measured an equilibrium constant, K_A, at $5.01 \pm 0.61 \times 10^9$ M^{-1}, a value similar to that of ^{125}I-NGA-44 (*9*). The reverse binding rate constant, k_{-b}, for DF-NGA-41 was $1.22 \pm 0.16 \times 10^{-3}$ min^{-1}, which was equal to the k_{-b} of ^{125}I-NGA-44. Based on K_A and k_{-b}, the forward binding rate constant, k_b, was calculated to be $6.11 \pm 1.07 \times 10^6$ M^{-1} min^{-1}.

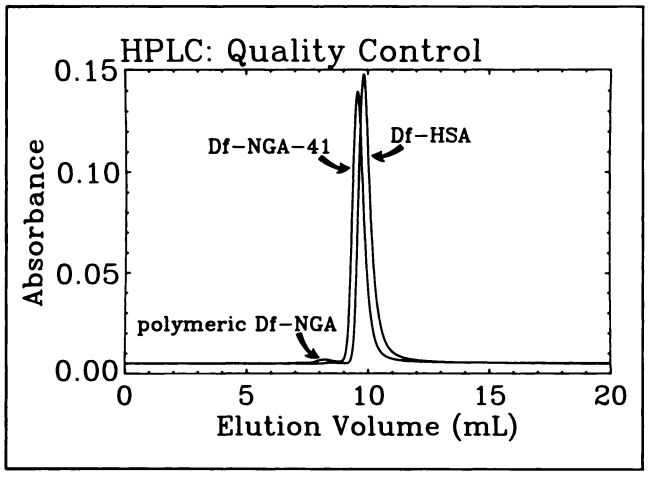

FIGURE 2. Size-exclusion chromatography of DF-HSA with 0.70 DF per HSA and DF-NGA-41 with 1.1 DF per NGA revealed minimal polymerized product.

Biodistribution

Tissue uptake for ^{67}Ga-DF-NGA-41 (1.1 DF per NGA) and ^{125}I-HSA in %ID and %ID/gram of various tissue are listed in Table 1. At 3 min postinjection, liver and blood activity summed to within 13% of the injected activity. Only the liver, urine, small intestine contents and large intestine contents contained more ^{67}Ga than ^{125}I activity; the ^{67}Ga activity within the latter three organs was less than 2% of the ID. At 60 min, the liver, small intestine, small intestine contents, stomach contents and urine contained more ^{67}Ga than ^{125}I activity. The urine and small intestine contents, which accumulate the hepatic metabolites of ^{99m}Tc-NGA (*1,10*), contained 7% and 2% of the injected ^{67}Ga, respectively. The urinary bladder, eyes and gonads contained less than 1% of the ID at the 3- and 60-min time points. The liver retained most of its ^{67}Ga activity with 42%–58% of the ID still present at 60 min.

Gallium-labeled DF-NGA displayed dose-dependent kinetics (Fig. 3). The rate of DF-NGA uptake by the liver differed for each scaled molar dose. These curves were similar to those generated by similar scaled molar doses of ^{99m}Tc-NGA (*10*) (Fig. 3). Increasing the scaled molar dose decreased the rate of hepatic uptake and increased the time required to reach maximum activity. The smallest dose, 1.2×10^{-9} mol/kg, peaked in the liver at approximately 5 min representing 85% of the ID.

Dosimetry

The absorbed radiation doses in units of rad per mCi were: liver, 1.6; small intestine, 0.74; urinary bladder wall, 1.5; total body, 0.049; red marrow, 0.017 ovaries, 0.038; uterus, 0.058; and testes, 0.016. The absorbed dose to the lens of the eye was considered equal to the total body dose.

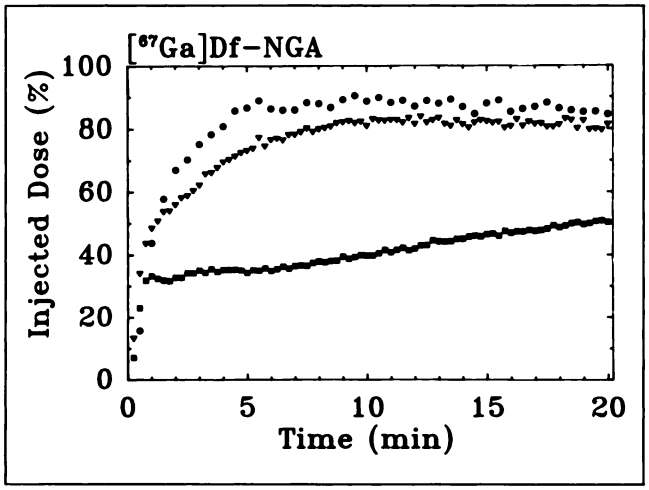

FIGURE 3. Gallium-67-DF-NGA displayed dose-dependent uptake in rabbits. The three scaled molar doses were: 1.2×10^{-9} mol/kg (30 sec/fr) (circles), 1.2×10^{-8} mol/kg (diamonds), and 1.2×10^{-7} mol/kg (squares).

This was based on the lack of active ^{67}Ga-DF-NGA uptake in the eye (Table 1) at 3 and 60 min postinjection.

DISCUSSION

The purpose of this work is two-fold: (a) to establish the biochemical similarity of gallium-labeled DF-NGA with ^{99m}Tc-NGA, and (b) to determine the compatibility of ^{68}Ga-DF-NGA PET imaging with the kinetic model. Three criteria can be used to determine the biochemical similarities and the potential for kinetic modeling via PET imaging: standard, receptor binding and modeling.

Standard Criteria

The choice of ^{68}Ga was based on the convenience and relatively low cost provided by ionic ^{68}Ge/^{68}Ga generators (*13*). Two additional advantages of ^{68}Ga are the 68-min half-life, which is compatible with NGA kinetics, and the ability to perform biodistribution and in vitro assays with ^{67}Ga-labeled DF-NGA. One disadvantage of ^{68}Ga is a high beta emission energy which results in diminished spatial resolution and less favorable dosimetry. Dosimetry calculations indicate the liver as the critical organ with 1.6 Rad per mCi of administered ^{68}Ga-DF-NGA. Using a standard ^{99m}Tc-sulfur colloid SPECT study as a basis (8 mCi, 2.8 rad) (*14*), an equivalent absorbed dose to the liver would result from 1.75 mCi of ^{68}Ga-DF-NGA.

Selection of deferoxamine as the bifunctional chelator was based on its selectivity for Ga^{3+}, high affinity, and coupling reactivity. As outlined by Yokoyama (*7*), when chelation of Ga^{32+} is sought, deferoxamine has several advantages over derivatives of DTPA. First is ionic selectivity, where the chelator has extremely low affinity for zinc, copper and manganese cations (*15*), trace metals of significant physiologic import. An important concern expressed by Wagner and Welch (*16*) is in vivo stability of the gallium chelate with respect to iron-binding proteins such as lactoferrin and transferrin. This has been addressed by Weiner et al. (*17*) with the conclusion that the DF-gallium chelate is stable in plasma. Additionally, deferoxamine is a true bifunctional reagent with three hydroxamate groups providing a six coordinate complex with Ga^{3+}, and a reactive amino group for coupling to the protein. Thus, unlike most DTPA derivatives, attachment of DF to proteins does not require the loss of a coordinate position. Lastly, a motivation for deferoxamine is an extensive clinical experience as the agent of choice for iron-chelating therapy (*18*). A standard imaging protocol (70-kg subject) will require a DF-NGA dose of 1.2×10^{-7} mole; the average DF density will be 1 DF per NGA. This is equivalent to 10^{-4}th of a single deferoxamine dose (1.5×10^{-3} mole) for chelation therapy.

Two methods were available which utilize different amino acids on the protein. Carbodiimide activation (*19*) of the DF primary amine uses carboxyl residues to form an amide linkage to proteins. An alternative was the two-step glutaraldehyde described by Yokohama (*7*), which utilizes the ϵ-amine of lysine. Because the galactosyl bifunctional reagent, IME-thiogalactose (*1*), also uses an amidine linkage to the lysine residues of albumin, we initially selected (*6*) the carbodiimide method. Different attachment sites for each bifunctional agent would permit the synthesis of DF-NGAs with the maximum number of galactose units per albumin macromolecule. Unfortunately, the carbodiimide method was unsatisfactory. Control of the reaction pH was not precise and led to wide variations in DF-to-NGA ratios. More significant, was the lack of apparent DF coupling stability. Storage at 5°C for a week would result in a decrease (~5%) in the DF-to-NGA ratio and substantially diminished labeling yields. For these reasons, the two-step glutaraldehyde method was attempted with superior results. The DF-to-NGA ratios were reproducible and were stable with respect to long-term storage.

An initial concern with the glutaraldehyde method was the possibility of NGA polymerization. As illustrated in Figure 2, polymerization was minimal with DF coupling reactions that produced DF-NGA ratios of approximately 1:1; a ratio that provided quantitative labeling yields. The disadvantage of sharing the lysine residues for attachment of both bifunctional agents was the variation in DF coupling conditions with NGA carbohydrate density. As illustrated in Figure 1, an NGA with 41 galactose units per HSA required five times the ratio of DF-to-protein than native HSA which has no galactose residues. Lastly, the two-step glutaraldehyde method is amenable to scaling up. The reactant ratios used in Figure 1 produced similar DF-to-NGA ratios when the reaction volume and reactant quantities were increased by a factor of five.

Receptor-Binding Criteria

The in vitro and biodistribution assays were performed to measure the receptor-binding properties of the new radiopharmaceutical, DF-conjugated NGA. These properties, which can be characterized (*10*) in terms of specificity and saturability, should not differ from the parent agent, radiolabeled-NGA. Similar affinities (K_A) of ^{67}Ga-DF-NGA and ^{99m}Tc-NGA indicate that attachment of the chelator preserved the molecular specificity of the NGA-receptor interaction. One factor that minimizes structural alteration of NGA by deferoxamine is an absence of charge on the chelator at a neutral pH. Additionally, attachment of the chelator should not alter the biodistribution of the ligand. Two observations confirm this requirement. First, the biodistribution of ^{99m}Tc-NGA (*1*) and DF-coupled NGA are similar (Table 1). Second, ^{67}Ga-DF-HSA exhibits a slightly slower (10%) plasma clearance of ^{131}I-HSA (*7*).

Saturability was also preserved. This was demonstrated by a progressive decrease in hepatic uptake with increasing scaled molar doses of ^{67}Ga-DF-NGA (Fig. 3). Similar dose-dependent uptake was observed with ^{99m}Tc-NGA (*10*). At the two lowest scaled molar doses (1.2×10^{-9}, 1.2×10^{-8} mole/kg) ^{67}Ga-DF-NGA reached a maximum within the

liver prior to 15 min postinjection. The highest molar dose reached maximum at approximately 20 min postinjection. This dose saturated the available receptor sites. Consequently, the maximum hepatic accumulation of approximately 50% ID represents an equilibrium of a reversible bimolecular reaction at saturation. Saturability of the receptor by DF-NGA has significant modeling implications; preliminary simulations of a regional model predict that high precision estimates of receptor density will require at least 50% saturation of the receptors within the region.

Modeling Criteria

Regional measurements of receptor biochemistry will require a kinetic model. Successful modeling via PET imaging will require adequate count rates and recoveries from plasma and liver. Using the ECAT EXACT (Siemens, Chicago, IL) as an example predicts that a 1.75 mCi injection of ^{68}Ga-DF-NGA will yield ample counting statistics. Based on a sensitivity of 220 kcts/μCi/sec/ml, 1.75 mCi would produce ~230 kcts/sec per ml of liver (volume ~1.5 liters) at peak uptake, which usually represents 90% of the dose when a healthy organ is imaged (*4*). Setting a bin size of 15 sec provides a data point with 3500 kcts per 1 ml of tissue at peak liver activity, which has a relative error of less than 0.1%. Consequently, the counting error is far smaller than that produced by patient motion and respiration, which is about 2–4% using 15 sec sampling intervals (*20*). The high counting rate will have two advantages. First, a narrow bin size of 1 sec could be used to minimize effects of patient motion and respiration. Second, hepatic disease can diminish receptor density to 20%–30% of normal (*20*). Therefore, hepatic time-activity data should have a count rate five times higher than optimum for normal tissue. This precaution would allow adequate count rates within regions of defective receptor biochemistry.

An additional consideration is the method by which the plasma clearance data is sampled. Three alternatives are possible: (a) multiple blood samples, or tomographic data from (b) the right ventricle, or (c) the abdominal aorta. Of the three methods, multiple blood sampling during the 30-min imaging study is highly undesirable. Sampling from tomographic data should be possible. Modeling of ^{99m}Tc-NGA utilizes plasma data from 3 to 15 min postinjection. During this time interval, the %ID of NGA declines from ~50% to ~20% of the dose. Assuming a 70-kg subject, this translates to time-activity data which spans 65 kcts/sec/ml of plasma to 26 kcts/sec/ml during the 12-min interval. Due to greater rigidity and minimal motion the aorta would be the preferred site. Additionally, sampling from the abdominal aorta would free the entire axial field of view (FOV) for observation of the liver. The ECAT EXACT with an axial FOV of 16.2 cm could therefore view the entire liver. This observational scheme (assuming correction for slice overlap) would permit conservation of mass within the kinetic model; a requirement for high precision estimates of regional receptor concentration and affinity (*6*).

The optimal data set would be attenuation-corrected plasma and liver time-activity curves in units of cps/volume, which would then be converted (via a counting standard) to mole/volume of NGA. Sampling of plasma data from the upper abdominal aorta will require complete recovery of the count density within the vessel. This can be achieved when the diameter of the vessel is greater than 2.7 times the FWHM of the tomograph (*21*). The use of 0.7 as a typical FWHM yields a minimum diameter of 19 mm. Depending on the method, diameter measurements of the thoracic abdominal aorta vary from 1.4 (*22*) to 2.6 mm (*23*). Therefore, a cautious approach would allow a calibration of the aortic ROI data with a single (or duplicate) i.v. plasma sample.

Significance

The liver is often referred to as the "silent organ." Chronic diseases, such as hepatitis and cirrhosis, remain silent during years of progression. During this time, clinical tests are insensitive and clinical histories can be of dubious value. There exists a set of anecdotal observations that suggests a regional origin of chronic liver disease (*24*). However, without a noninvasive test of regional hepatic function, this hypothesis remains untestable. Consequently, a positron-emitting receptor-binding radiopharmaceutical, such as ^{68}Ga-DF-NGA, will provide a small window into the most complex of biochemical processors, the human liver.

ACKNOWLEDGMENTS

The author is grateful to Dr. Akira Yokoyama for his thoughtful review of the manuscript and for the deferoxamine assay protocol, and Drs. William C. Eckelman, Robert C. Stadalnik, Landis K. Griffeth for their comments. The author thanks Kathleen Ratcliff and Theodore Barlow for their excellent technical assistance. This work was supported by PHS grant RO1-AM-34768 from the National Institute of Diabetes and Digestive and Kidney Diseases.

REFERENCES

1. Vera DR, Stadalnik RC, Krohn KA. Technetium-99m-galactosyl-neoglycoalbumin: preparation and preclinical studies. *J Nucl Med* 1985;26:1157–1167.
2. Stadalnik RC, Vera DR, Woodle ES, et al. Technetium-99m-NGA functional hepatic imaging: preliminary clinical experience. *J Nucl Med* 1985;26:1233–1242.
3. Kudo M, Vera DR, Stadalnik RC, et al. In vivo estimates of hepatic binding protein concentration: correlation with classical indicators of hepatic functional reserve. *Am J Gastroenterol* 1990;85:1142–1148.
4. Vera DR, Stadalnik RC, Trudeau WL, Scheibe PO, Krohn KA. Measurement of receptor concentration and forward binding rate constant via radiopharmacokinetic modeling of technetium-99m-galactosyl-neoglycoalbumin. *J Nucl Med* 1991;31:1169–1175.
5. Kudo M, Vera DR, Trudeau WL, Stadalnik RC. Validation of in vivo receptor measurements by in vitro radioassay: technetium-99m-galactosyl-neoglycoalbumin as a prototype model. *J Nucl Med* 1991;31:1177–1182.
6. Vera DR, Krohn KA, Stadalnik RC, Scheibe PO. Error analysis of regional

measurements of hepatic receptor biochemistry via PET observations of [^{68}Ga]-deferoxamine-galactosyl-neoglycoalbumin kinetics. *J Label Comp Radiopharm* 1989;26:348–350.
7. Yokoyama A, Yoshiro O, Horiuchi K, et al. Deferoxamine, a promising bifunctional chelating agent for labeling proteins with gallium: Ga-67-DF-HSA. *J Nucl Med* 1982;23:909–914.
8. Emery T, Hoffer PB. Siderophore-mediated mechanism of gallium uptake demonstrated in the microorganism *Ustilago sphaerogena*. *J Nuc Med* 1980;21:935–939.
9. Vera DR, Krohn KA, Stadalnik RC, Scheibe PO. Tc-99m-galactosyl-neoglycoalbumin: in vitro characterization of receptor-mediated binding. *J Nucl Med* 1984;25:258–261.
10. Vera DR, Krohn KA, Stadalnik RC, Scheibe PO. Tc-99m-galactosyl-neoglycoalbumin: in vivo characterization of receptor mediated binding to hepatocytes. *Radiology* 1984;151:191–196.
11. Emery T. Exchange of iron by gallium in siderophores. *Biochemistry* 1986; 25:4629–4633.
12. Snyder WS, Ford MR, Warner GG, Watson SB. "S" absorbed dose per unit cumulative activity for selected radionuclides and organs. *MIRD pamphlet no. 11*. New York: The Society of Nuclear Medicine; 1975: 92–93.
13. Green MA, Welch MJ. Gallium radiopharmaceutical chemistry. *Nucl Med Biol* 1989;16:435–448.
14. MIRD dose estimate report no. 3: summary of current radiation dose estimates to humans with various liver conditions from Tc-99m sulfur colloid. *J Nucl Med* 1975;16:108A.
15. Simon P, Ang KS, Meyrier A, Allain P, Mauras Y. Desferrioxamine, oculary toxicity, and trace metals. *Lancet* 1983;8348:512–513.
16. Wagner SJ, Welch MJ. Gallium-68 labeling of albumin and albumin microspheres. *J Nucl Med* 1979;20:428–433.
17. Weiner RE, Thakur ML, Goodman M, Hoffer PB. Relative stability of In-111 and Ga-67 desferrioxamine and human transferrin complexes. In: Sodd VJ, Hoogland DR, Ice RD, Sorensen JA, eds. *Radiopharmaceuticals II: proceedings of the 2nd international symposium on radiopharmaceuticals*. New York: The Society of Nuclear Medicine; 1979:331–340.
18. Hershko C, Weatherall DJ. Iron-chelating therapy. *CRC Crit Rev Clin Lab Sci* 1988;26:303–345.
19. Janoki GA, Harwig JF, Chanachai W, Wold W. [^{67}Ga]deferoxamine-HSA: synthesis of chelon protein conjugates using carbodiimide as a coupling agent. *Int J Appl Radiat Isot* 1983;34:871–877.
20. Vera DR, Scheibe PO, Krohn KA, Trudeau WL, Stadalnik RC. Goodness-of-fit and local identifiability of a receptor-binding radiopharmacokinetic system. *IEEE Trans Biomed Eng* 1992;BME-39:356–367.
21. Kessler RM, Ellis JR Jr, Eden M. Analysis of emission tomographic scan data: limitations imposed by resolution and background. *J Comput Assist Tomogr* 1984;8:514–522.
22. Aleksandrowicz R, Gosek M, Provok M. Normal and pathologic dimensions of the abdominal aorta. *Folia Morphol* 1974;33:309–315.
23. Leithner C, Sinzinger H, Hoheneoker J, Wecke L, Olbert F, Feigl W. Radiologic anatomy of the abdominal aorta and their large branches. *Okajimas Fol Anat* 1975;52:119–150.
24. Greenway CV, Stark RD. Hepatic vascular bed. *Phys Rev* 1971;51:23–65.